




## Simplified model for dam rockfill creep and influence of constructive delay of concrete face

Renato Santos Paulinelli Raposo<sup>1#</sup> , Yasletty Zamora Hernández<sup>2</sup> ,  
André Pacheco de Assis<sup>1</sup> 

Article

### Keywords

Concrete Face Rockfill Dams  
Creep  
Slab

### Abstract

Advances in equipment and tools implemented for geotechnics have been allowing design to be supported by numerical simulations. However, even with sophisticated resources, the dam geotechnical engineering industry still lacks few information on laboratory parameters as in the case of Concrete Face Rockfill Dams (CFRD). It is necessary to simplify the use of back-analysis that represent real CFRD, in search of tools that can be applied in the industry. The objectives include the simplification of the behavior of the linear modules associated with a linear coefficient representing the vertical creep and evaluation of the influence of the constructive delay of the concrete face in a specific case. The text goes through examples of real CFRD simulations, as a theoretical background. The CFRD calibration model includes an elegant representation of the vertical orthotropic rockfill creep with only two calibration parameters. The displacements obtained from a CFRD are represented with a linear elastic constitutive model with linear vertical deformation in time. The result is well adjusted both in the construction phase and during filling. Further on, six different slab constructive delay sequencing arrangements were simulated. The study uses a numerical device that makes it possible to drive the concrete slab in its correct design thickness. Among the stress results, the step-by-step sequencing of the slab following the rockfill reached the worst horizontal stresses, reaching almost 45 MPa, which exceeds the typical compressive strengths of conventional concretes that can affect the structural integrity of the slab. The results suggest that step-by-step sequencing should be avoided. In the case studied, the balanced behavior could be achieved in a concreting scenario maintaining the constructive delay of the slab with at least half the height of the dam. It is important to point out that all this work considerations serve for a specific example. Any generalization should be avoided or associated with broader complementary studies, as each dam is a unique work and must be studied individually, case by case.

## 1. Introduction

Concrete-faced rockfill dams (CFRD) have proven to be quite safe in terms of slope stability, commonly with safety factors above seven. Robustness is also evidenced in seismic zones, as the rockfill does not develop additional pore pressures under these conditions (ICOLD, 2010). For example, when an earthquake measuring 8 on the Richter scale occurred in 2008, the epicenter was about 20 km away from the 156 m-high Zipingpu Dam in China, which stood firm. Despite some localized damage to the slab and crest, the structure remained safe and stable (Cruz et al., 2014). ICOLD (2010) cites some examples of problems not related to rockfill masses, such as: foundation erosion due to overtopping, regressive internal tubular erosion (piping) of

the foundations or failures in hydraulic mechanisms such as spillways, water intakes, diversion galleries etc. Even with advances in numerical simulation methods, rockfill dam designs require many simplifications, mainly due to difficulties in laboratory tests on larger particle sizes. In general, it is practically impossible to obtain the material properties by direct methodology. Its dimensioning involves complex phenomena of water propagation over time and its criteria are predominantly semi-empirical (Pinto, 2007). The problem may be more complex when the material is not completely flooded, as in the case of CFRD. Deformation arrangements not foreseen in the design generated surprising cases of large ruptures in sealing slabs. Over the last few decades, advances in equipment and tools implemented for geotechnics are increasingly allowing projects to be supported by numerical

<sup>#</sup>Corresponding author. E-mail address: renatopaulinelli@gmail.com

<sup>1</sup>Universidade de Brasília, Departamento de Engenharia Civil e Ambiental, Brasília, DF, Brasil.

<sup>2</sup>Universidade Estadual do Norte Fluminense, Laboratório de Engenharia Civil, Campos dos Goytacazes, RJ, Brasil.

Submitted on August 8, 2021; Final Acceptance on June 21, 2022; Discussion open until November 30, 2022.

<https://doi.org/10.28927/SR.2022.074221>



This is an Open Access article distributed under the terms of the Creative Commons Attribution License, which permits unrestricted use, distribution, and reproduction in any medium, provided the original work is properly cited.

simulations. Several works have used numerical simulations to study the types of failure and the main causes of failure of these dams (Chen et al., 2019; Pramthawee et al., 2017; Wei & Zhu, 2015; Xavier et al., 2007; Yao et al., 2019; Zhang et al., 2004; Zhou et al., 2016). However, the availability of advanced and sophisticated resources may take time to reach the dam geotechnical engineering industry.

The difficulty in forecasting new projects reinforces the growing trend to revise design criteria using back analysis based on technical bases based on the performance of previous works. The creep of the CFRD rockfill develops throughout construction, during filling and later in the operation of the dam. The main motivation of the study is based on the search for simplicity in a constitutive model that can represent the behavior reality of rockfill creep. The technical means have expanded the database on the deformability behavior of rockfills, before, during and after filling the reservoir.

Dams are checked over time. As main information: the vertical and horizontal displacements within the embankment, crest settlements and displacement readings of the slabs during the first filling. Even with the volume of data checked, according to Basso (2007), the constitutive laws are unrealistic in relation to the data read in the field, due to different rockfill regions if the construction phases are considered. The constructive stresses are low near the sides of the backrests and the filling of the reservoir promotes a rotation of stress mainly in the first third of the upstream slope. The main objective of the present work is to propose and validate a consolidated calibration methodology for rockfill creep applied to dams with a concrete face that considers deformability in time and propagated flow of reservoir filling from the back analysis of Swedish boxes and displacements in the slab. The deformability behavior of rockfill is treated by its macroscopic phenomena with two main parameters of a simplified constitutive model: deformability modulus and creep that depend on time, wetting and stress magnitude.

### 1.1 Collapse and creep in rockfill

The use of three-dimensional simulations for CFRD projects is a practice that is spreading recently. According to a study by Frutuoso (2007), most designs were built with two-dimensional simulations and linear elastic models. This practice ends up ignoring the influence of the effect of the shoulder and the non-linearity of geotechnical materials. According to Naylor et al. (1981), the ideal model to simulate CFRD would be:

- Non-linear stress-strain relationships
- Several stress paths
- Time effect, with deformations such as consolidation and creep
- Anisotropy, especially in compacted soils
- Dilatancy, as shear stresses can also cause volume increase
- Increased material stiffness during loading.

The criteria proposed by Sherard & Cooke (1987) continue to be followed by most designers today, nearly thirty years after publication. Cost and schedule challenges have forced bolder projects and advances in three-dimensional analysis help to adapt to classical criteria.

### 1.2 Compressibility model for rockfill

The one-dimensional model was proposed by Oldecop & Alonso (2001), which has the proposal to represent rockfill deformability. The breakage and rearrangement of rockfill particles depend not only on the acting stresses, but also on the relative air humidity conditions, which fills the gaps in the rock blocks. The great contribution of this work is the observation that the rockfill collapse in environments with 100% relative air humidity is the same as observed in flooded samples. According to the authors, rockfill has an intrinsic dependence on deformation over time and the crack propagation speed in general has two main variables: stress level and moisture content. The rock pores can have a determining influence on the deformability of rockfills. The work of Oldecop & Alonso (2003) complemented the model with the addition of new results of controlled consolidation tests. Improvements in its constitutive equations generated gains in the formulation, such as the correction of a hardening that does not depend on the initial formulation and has an excellent adherence to experimental results.

Oldecop & Alonso (2007) demonstrated that the long-term behavior of deformations can be linear in relation to the logarithm of time, if the materials are granular and the consolidation tests are long-term in large diameters. The macroscopic behavior can be explained from the phenomenon of crack propagation, with successive breakage of grains subjected to stress, whose microcracks are influenced by issues such as relative humidity.

## 2. Proposed Rockfill deformability modeling in CFRD

The proposed deformability model considers two mechanical parameters to be calibrated: a constant deformability modulus ( $E$ ) in the MPa unit and an additional constant deformation percentage in the vertical direction during construction (creep) in the %/year unity.

The stress and deformation response of the model follows the linear elastic modulus, which takes the proposal of deformability over time to a very simple level. The purpose of this interpretation is to verify the possibility of adjusting the deformability of the slab before and during filling, even in a linear elastic model. The Young's modulus represents the isotropic deformability with the linear-elastic ABAQUS® Mechanical model, Elasticity.

The paper does not use the hyperbolic model, even though it is widely used to represent the behavior of rockfill.

Also, the transverse anisotropic nature of the rockfill was not considered. These are simplifying assumptions due to the indication of satisfactory results between read and measured vertical displacements with elastic deformability and creep models. The model is complex due to the three-dimensional geometry that involves stepwise construction and finite element mesh separation.

The additional parameter in the vertical direction is linked to the control variable ( $S'$ ), which controls the forced reduction of the vertical volume. The range is between 0 and 100%, in the percentage missing in relation to the total of the parameter during construction. This is implemented as orthotropic thermal expansion in the vertical direction, since the variable  $S'$  is the temperature in the ABAQUS® Mechanical model, Expansion. During construction, this constructive fluency follows a line in time as a boundary condition:

$$S'(t) = 1 - \frac{t - t_0}{t_f - t_0} \quad (1)$$

Where:

$S'$  = control variable for missing percentage of creep [dimensionless]

$t$  = constructive time variable [time];

$t_0$  = construction start time constant [time].

$t_f$  = time constant at the end of construction [time].

The other parameters are arbitrated and constant:

- Poisson values were adopted with a value of 0.3, including for slab and plinth
- the concrete material is linear elastic with Young's Modulus adopted as 20 GPa
- the unit weight is 20 kN/m<sup>3</sup> for rockfill and 25 kN/m<sup>3</sup> for concrete

- the heat flux arbitrated values of 100 K·m·W<sup>-1</sup> for thermal conductivity and 1 J·K<sup>-1</sup>·kg<sup>-1</sup> for specific heat, which does not influence the analysis at all, because the temperature variation is imposed.

In this work it was chosen not to add any shear strength to the models, assuming that the CFRDs have no recent history of slope instability.

## 2.1 Geometry

The geometry of the dam model is based on previous study presented by Raposo (2016), maintaining aspects as height (200 m), shape of the valley, concrete face thickness, width of the berm, dimensions of the plinth, slopes. Only half of the model is mounted. The dam geometry is separated into three major fundamental parts shown in Figure 1, the rockfill dam body (white), a replaceable rockfill face layer (blue) and the slab (grey). The image also defines the Swedish boxes positions (red circle) and horizontal construction lines, each with a 10 m lift.

In addition to the X, Y and Z axes, a rotated reference is defined, where the Y' and X' plane is parallel to the shoulder plane. The vertical plane perpendicular to the Axis Z is sliced with 16 out of 16 m, propagates through the entire model. The slab thickness followed empirical criteria like those adopted for designing the Campos Novos and Barra Grande dams (Frutuoso, 2007). The thickness is reduced from the base to the top, with a change in the middle of the slab. The thickness adopted is 100 cm at the base, 50 cm in the middle and then 30 cm at the crest.

## 2.2 Interfaces and separation of materials

The ABAQUS® software allows mesh detachment between different parts, allowing differential movements

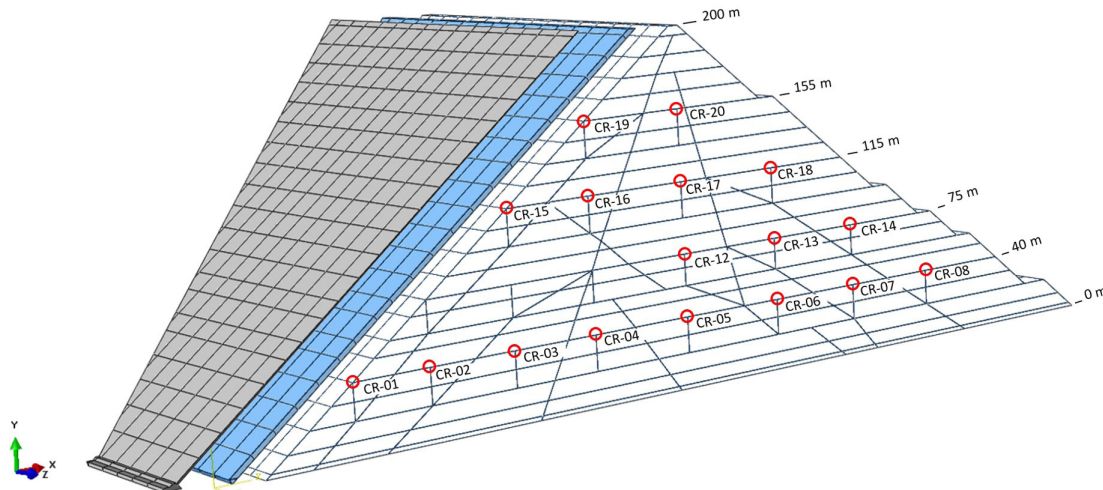


Figure 1. 3D geometry rockfill dam.

between the slab strips and between the slab and rockfill. The slab strips have a simply supported interface, both with its adjacent strip and with the blue layer and the plinth itself. According to the British Standard BS 5975 (BSI, 1996), the minimum value for the coefficient of friction in the contact between concrete/concrete and concrete/soil is 0.4, thus, it was adopted the value of friction at 0.5.

The blue layer in Figure 1 is divided into sets of 21 horizontal bands which composes a set. In each complete set it has bands stuck together with its adjacent one using the “tie” type interface. Each set, in turn, is also tied to the white part, joined with a “tie” type constraint. The interface between the rockfill dam body and the replaceable rockfill face layer is bonded with a “tie” type constraint. The interface between the concrete plinth and slab with the face rockfill replaceable layer is only a friction penalty of 0.5 as shown in Figure 2.

The regions are delimited from the Settlement Swedish Boxes (CR) shown by Cruz & Pereira (2007). To respect the

design and stress ranges, the areas of influence for each of the instrument regions were separated. The rockfills on the faces are the same as in the CR-01 region. The regions will be gradually grouped respecting the sectorization guidelines of Sherard & Cooke (1987) as presented in Figure 3.

### 2.3 Boundary and loading conditions

The boundary conditions of the three-dimensional model include displacement restrictions. The base of the model has three directions restrictions. The symmetry plane is restricted in the horizontal direction of the Y Axis. The abutment plane has a sectorization in the vicinity of the slab with restriction only in the normal plane (Z' axis) apart from a wider region with restriction in the normal and horizontal directions (Z' and X' axes), outside the region close to the slab. Reservoir filling is applied in five steps with conventional triangular hydrostatic diagram. Specific weight of water and gravity are rounded to 10 kN/m<sup>3</sup> and 10 m/s<sup>2</sup>.

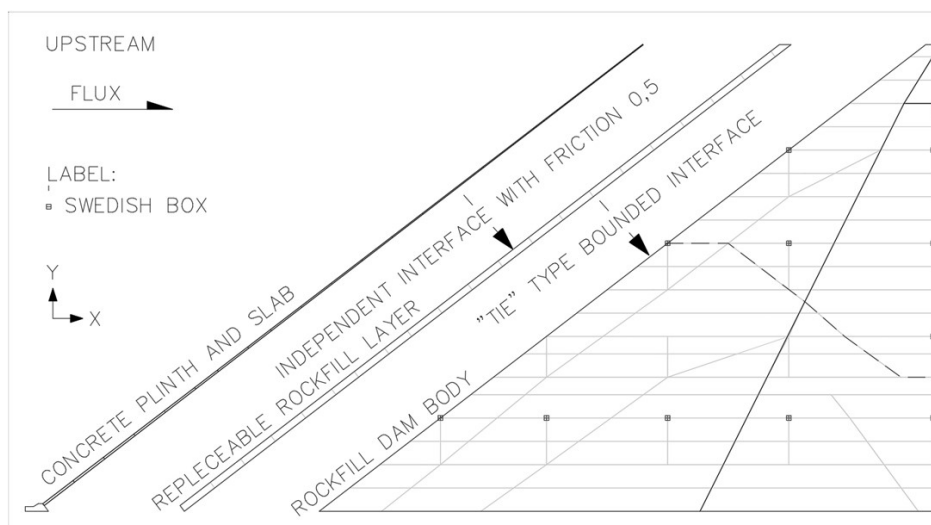


Figure 2. Interfaces between geometric parts.

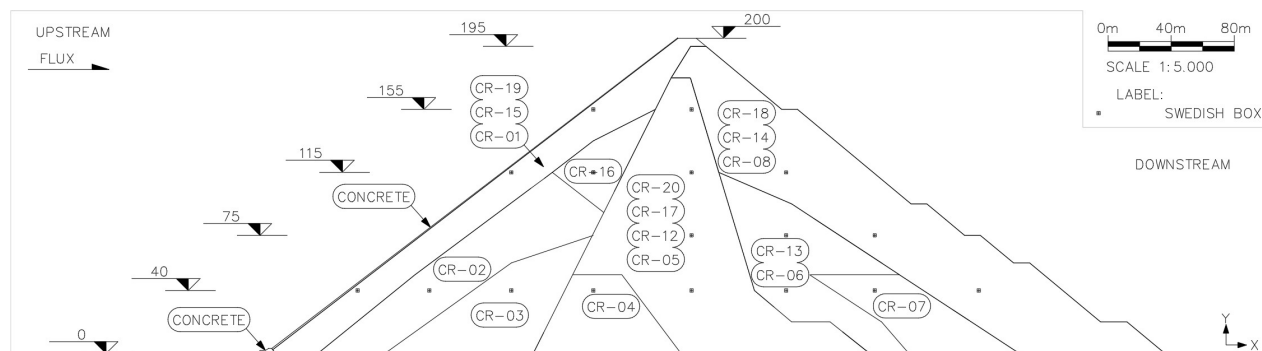


Figure 3. Geometric separation of materials.



## 2.4 Mesh

The tetrahedral rockfill elements are of the C3D4T type and the hexahedral concrete elements are of the C3D8R type, with approximate sizes of 5 m. The formulation of its matrix is coupled with temperature, transient and considering geometric nonlinearity with updating of the stiffness matrix at each increment. The mesh density study is not detailed here, but consisted in finding a finite element size based on the previous study presented by Raposo (2016).

## 2.5 Rockfill sequencing

The reference dam model was built in two phases, the first is highlighted in gray in Figure 4. In these analyses, the initial time is  $t_0 = 0$  days and the final time is  $t_f = 620$  days, as on Table 1, which are the input data for the imposition of vertical settlement in Equation 1. Raise times were based on the work by Cruz & Pereira (2007).

## 2.6 Slab construction delays

The study of the influence of the slab construction delay was carried out with six different scenarios, one by

one, arrangements of substitutions were being founded for each slab delay. The first scenario is named Step-by-step model, where the slab is activated following the dam body without initial embankment. The slab is activated with the rockfill at elevation 30 m. From then on, the slab is activated following each elevation step by step. The replacement of the sacrificial layer occurs level by level.

The second scenario is named 0/4 delay model. It considers a sectoring of the initial embankment (grey region in Figure 4), and the slab being activated step by step with the rockfill after the middle of the embankment. The three replacements of the rockfill surface layers start at step 13, as shown in Figure 5a. The first slab level is activated at step 14 and from on, the slab is lifted following the step-by-step embankment of the downstream slope.

The 1/4 delay model represents slab raising with the order of a quarter of the dam height, in relation to the rockfill raising. The five replacements of the rockfill surface layers start at step 18, according to Figure 5b. The 2/4 delay model represents slab raising with the order of half of the dam height. This model requires, at least, four replacements of the sacrificial rockfill surface layer, starting at step 23. The second, third and fourth replacements are at steps 27, 31 and 34, respectively, as shown in Figure 5c. The 3/4 delay

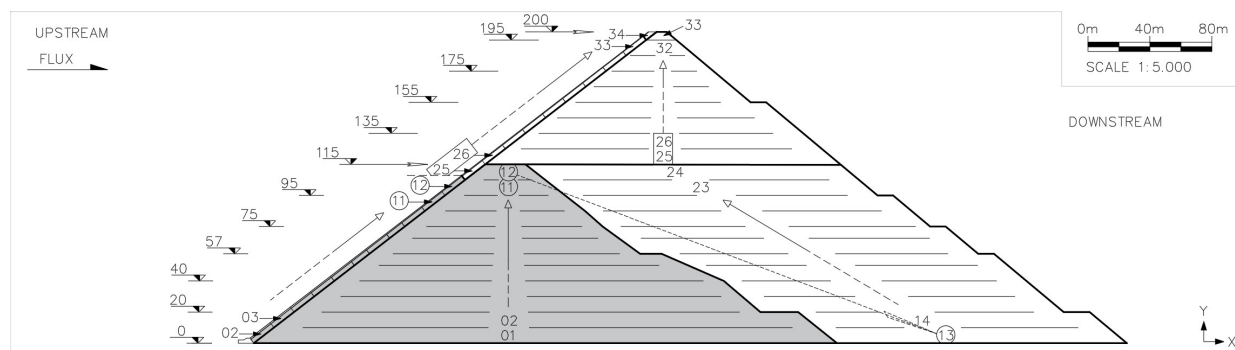


Figure 4. Standard elevation sequence from 01 to 34. Gray region first.

Table 1. Construction Steps of Rockfill.

First raise in gray (0 m to 115 m)			Downstream up to 115 m			Elevation above 115 m.		
Step	Height (m)	Days	Step	Height (m)	Days	Step	Height (m)	Days
1	010	10	13	115-010	230	25	125	380
2	020	30	14	115-020	240	26	135	440
3	030	50	15	115-030	250	27	145	480
4	040	70	16	115-040	260	28	155	520
5	050	90	17	115-050	270	29	165	540
6	057	110	18	115-057	280	30	175	560
7	065	130	19	115-065	290	31	185	580
8	075	150	20	115-075	300	32	195	600
9	085	170	21	115-085	305	33	200	610
10	095	190	22	115-095	310	34	Face Final	620
11	105	210	23	115-105	315			
12	115	220	24	115-115	320			

Simplified model for dam rockfill creep and influence of constructive delay of concrete face

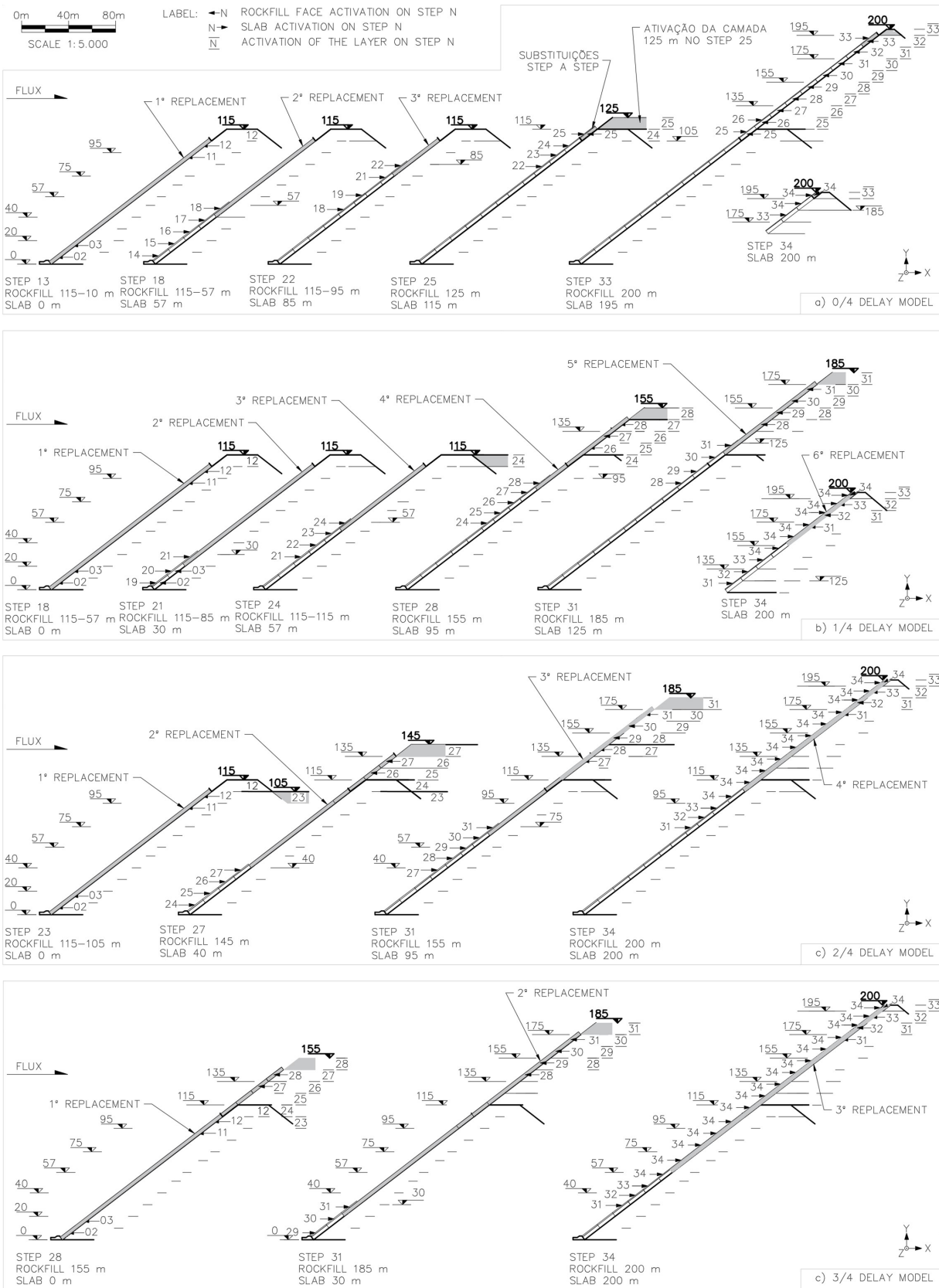


Figure 5. Sequencing of replacements and activation of the slab: (a) 0/4 delay model, (b) 1/4 delay model, (c) 2/4 delay model and (d) 3/4 delay model.

model represents raising the slab with the order of three quarters of the height of the dam. In this case, there were three replacements of the rockfill surface layers, according to Figure 5d. In the 4/4 delay model, the slab is only activated after the full height of the dam. Only two replacements of the rockfill surface layers were required in the last two steps.

### 3. Adjustments and calibration

The slab activation requires forced geometric adjustments that ensures activation of a concrete face with the correct thickness. The artifice consists of replacing a new layer on the rockfill face, with a completely new mesh (blue layer in Figure 1). Each replacement aligns the outer face with the original undeformed geometry. The inner face is fitted with the geometry already deformed from the fixed link (constraint: tie). The substitution generates a thickness change in the

rockfill face layer, that changes the stress field. Therefore, a second substitution is necessary to drive the slab in thickness to grant minimum residual stresses.

The vertical slab strips can move in independent directions with some friction between them. For future studies, it would be possible to think of some numerical implementation that adjusts the parametric activation of the slab thickness. The slab would have some differential curvature that follows the displacements of the rockfill base, maintaining the thickness.

#### 3.1 Slab thickness adjustment example

The concrete face sequencing used for calibration considers a slab delay of half of the dam height (2/4 delay model). Step 22 (Figure 6a) precedes the first replacement of the surface layer that occurs in the 23rd step (Figure 6b) without

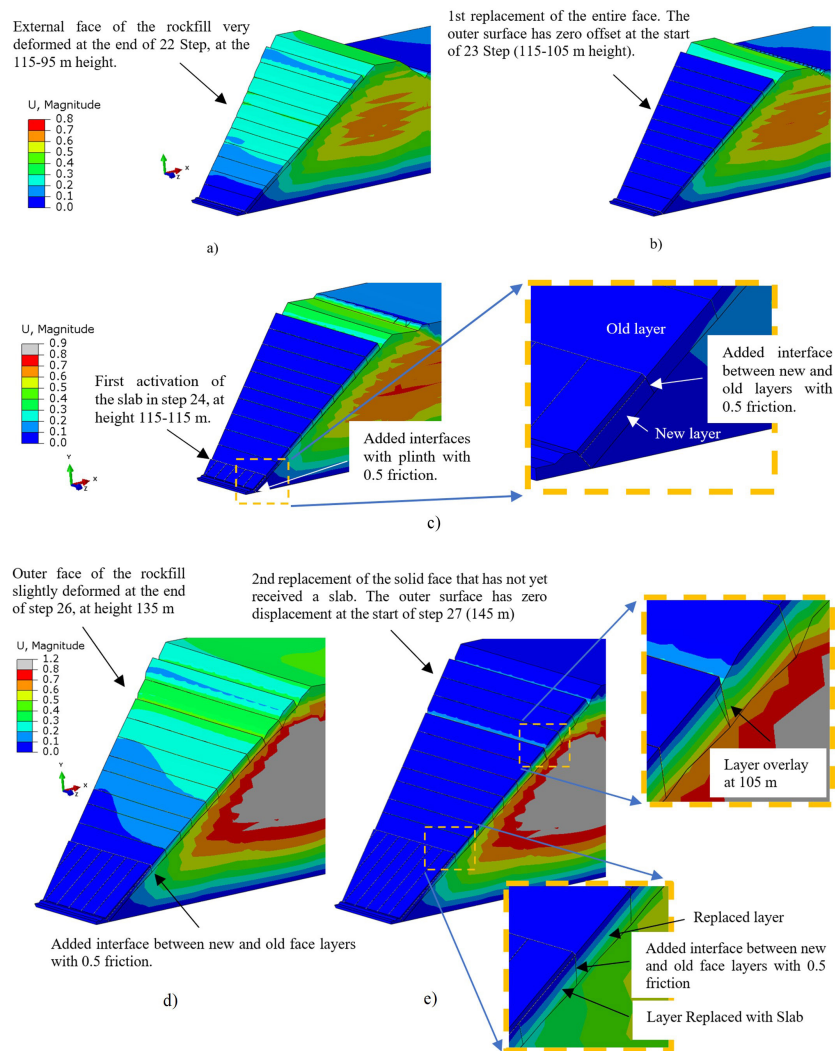


**Figure 6.** Replacing artifice, (a) step 22, before first replacement of the rockfill face and (b) step 23, showing face with zero displacement in 2/4 delay model. (c) activation of the first raising of the slab in step 24. (d) step 26, before second replacement and (e) step 27, adjusted face.

the concrete slab. The results images were extracted from the 2/4 delay model with ten times exaggeration. The slab starts to be activated in step 24 (Figure 6c), always in conjunction with the replacement of the rockfill surface layer immediately below and activation of the interface with the next layer. Step 26 (Figure 6d) presents accumulated displacements on the rockfill face, so the layer is replaced in step 27 (Figure 6e). A face remained linked to the previous displacement, creating an overlapping of layers at elevation 105 m. This condition was kept as it is because the sequential lifting of the slab does not reach the height of the inconsistency.

Step 30 precedes the third replacement of the surface layer. The inconsistency remains at an elevation of 105 m. The step 33 precedes the last activation of the slab, its level is at an elevation of 95 m. The activation of the rest of the slab in step 34 is still presented. The entire slab is activated at once.

### 3.2 Calibration Results

The calibration was obtained by a central section of the dam for the 1/2 delay model. The parameter results of Young Modulus ( $E$ ) and Vertical Deformation per year (creep) are shown in Table 2. According to the proposed methodology, Figure 7a and Figure 7b show the results of the calibrated model that compares the displacement curves obtained from Settlement Swedish Box (CR) with displacements calculated during the construction phase. Figure 8 shows the face displacement in the slab due to reservoir filling.

### 4. Stresses and displacements

Detailed stresses and displacements are shown only for the 1/2 delay model. The stress S33 is with a maximum in the order of 33 MPa (Figure 9a) and maximum total

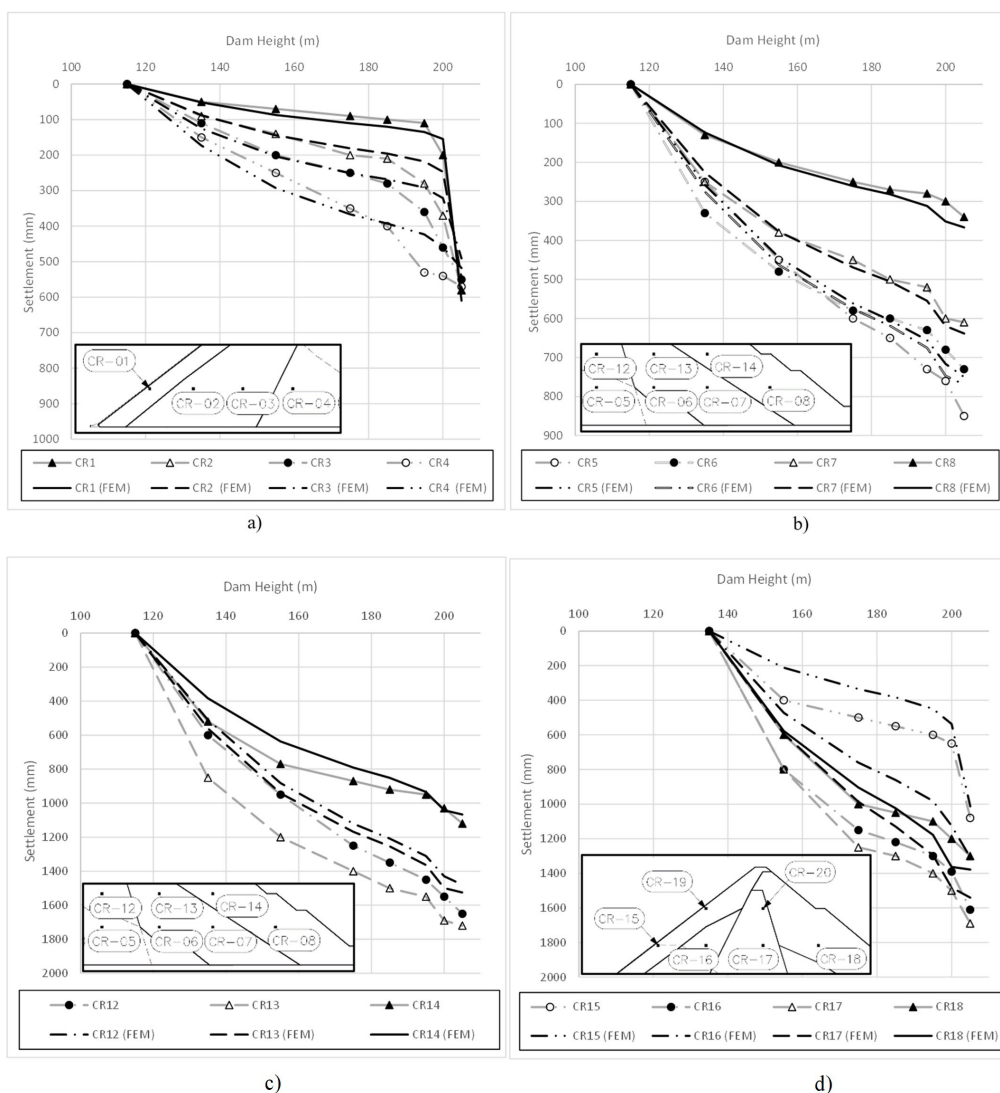


**Figure 7.** Displacements in the Swedish boxes positions (a) CR-01 to CR-04, (b) CR-05 to CR-08, (a) CR-12 to CR-14 and (b) CR-15 to CR-18. FEM calculated vs measured by Cruz & Pereira (2007).



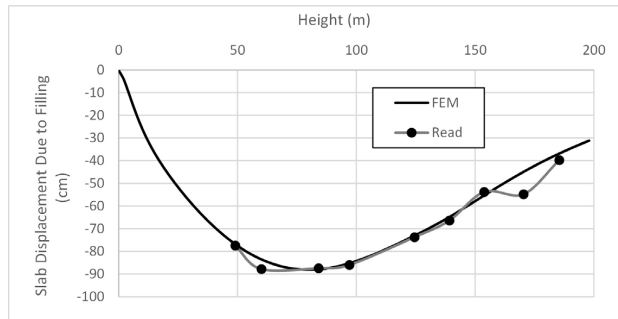


**Figure 8.** Displacement in the slab due to reservoir filling. FEM calculated vs measured from Xavier et al. (2007).

displacements in the order of 1 m (Figure 9b). Stress curves  $S_{11}'$  (longitudinal of the slab) get close to 6 MPa in the axis of symmetry (Figure 9c), except for the peaks of dimension 105 m. Transverse and shear stress curves are residual, without any suggestion for important bending moments. The curves in Figure 9d show the right axis displacement and the left displacement. The deviation is almost entirely in the range between -1% and 1%, slightly surpassing the range near the plinth.

All six scenarios show greater stresses in the shoulder-to-shoulder direction. Other stresses, including bending moment, are residual. Thus, the displacements (Figure 10a)

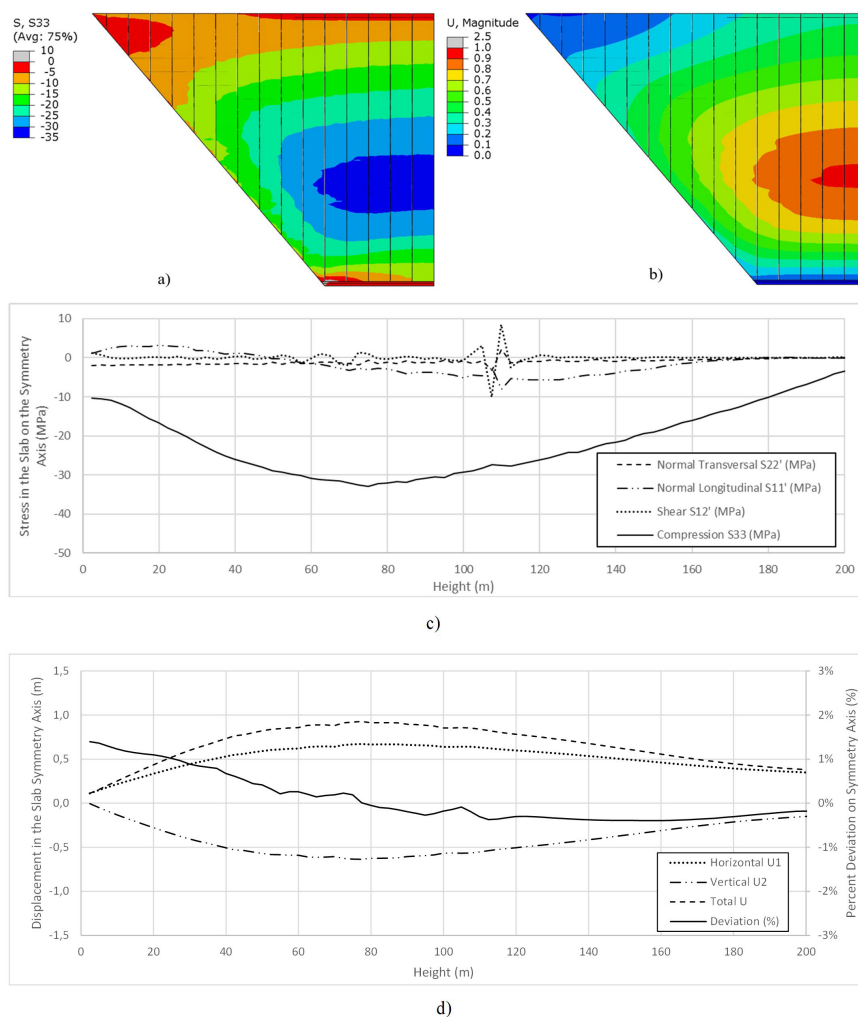


**Figure 9.** (a) horizontal stress  $S_{33}$  (MPa), (b) total displacements  $U$  (m), (c) slab stresses in the dam symmetry line (MPa) and (d) displacements (m) and deviation (%) in the slab in the dam symmetry line in the 2/4 delay model.

**Table 2.** Parameters calibrated using the 1/2 delay model.

REGION	UPSTREAM							CORE				DOWNSTREAM					
CR	01	15	19	02	16	03	04	05	12	17	20	06	13	07	14	18	08
$E$ (MPa)		80		100	80	100	180		180			80		80			80
Creep (%/year)		0		1	1.77	0.59	0.88		1.77			1.77		1.18			0.59

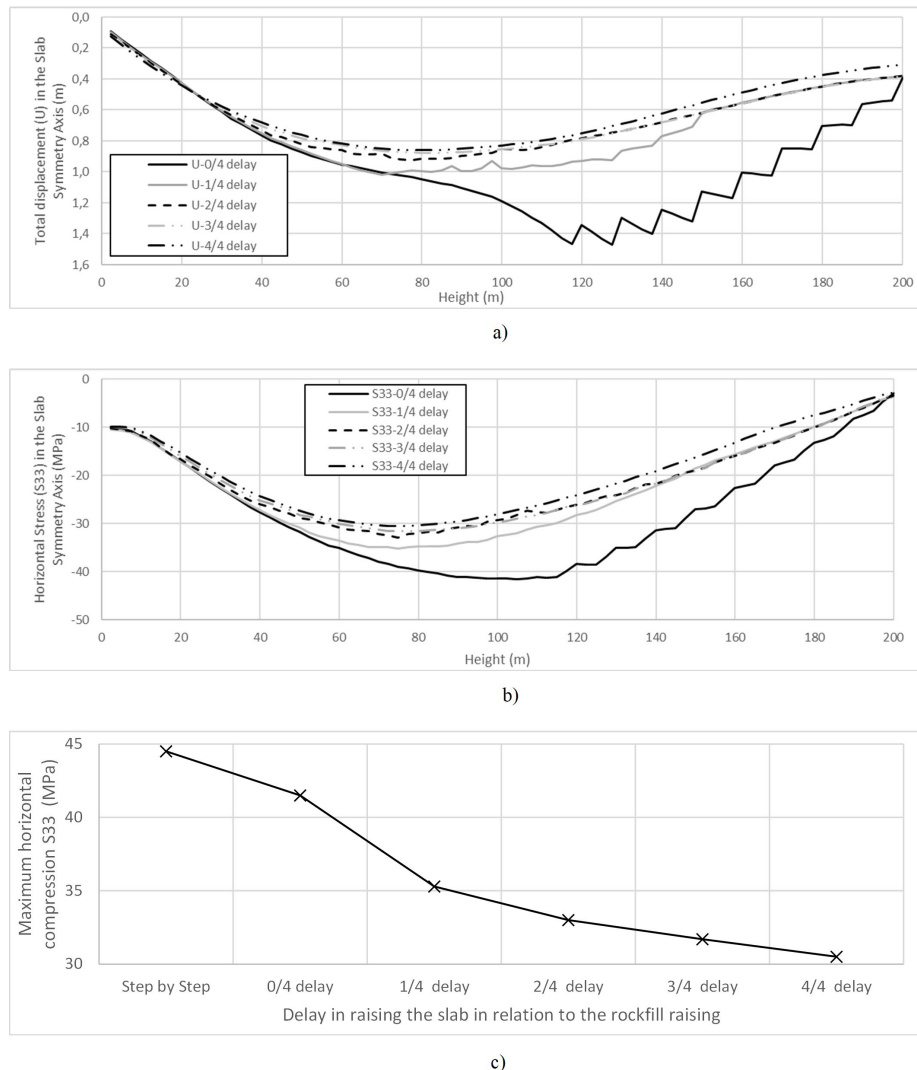


**Figure 10.** (a) Slab symmetry axis total displacement ( $U$ ) at five different slab delays, (b) slab symmetry axis horizontal compressions ( $S_{33}$ ) at five different slab delays, (c) synthesis of maximum results of horizontal compressions ( $S_{33}$ ) at six different slab delays.

and stresses  $S_{33}$  (Figure 10b) are presented comparing five different slab delays. All five scenarios start after the first gray landfill phase of Figure 4. In plot, it is noticeable that the curves with minor delay of the slab stand out from the others. Comparatively, it is possible to plot a synthesis of maximum horizontal stress in Figure 10c, including Step-by-Step. It is possible to observe that the presence of a greater reduction in stress  $S_{33}$  when there is a delay of at least a quarter of the slab in relation to the rockfill.

## 5. Conclusions

The forced linear reduction of vertical volume in time is implemented with a device of using orthotropic thermal expansion for coupling with linear mechanical behavior. Sophisticated constitutive models would involve an even greater difficulty for calibration. Furthermore, without massive

support of laboratory results, any more far-fetched results would inevitably fall back on a semi-empirical approach to estimating and fixing parameters that cannot be calibrated.

Restricted to the analyzed cases and starting from the purely behavioral view, the linear calibration presented a suitable result for the objectives of the work to serve as a basis for the sequencing studies. The worst sequencing arrangements would be step-by-step and zero delay where the slab strips are concreted, following each step of the rockfill raising. In these scenarios, stresses build up right at the beginning of the rockfill mass elevation. One of the models reached horizontal stress values that reach 45 MPa, which far exceeds the compressive strengths typical of conventional concretes. As highlighted, this expressive result becomes a point of attention regarding the structural integrity of the slab and this sequencing should really be avoided. The advantage of this condition could be associated with possible gains in terms

of a more closed work schedule, with some anticipation of filling the reservoir. This evaluation serves as a provocation that may suggest induction of cracking in the slab.

At least, all considerations need to be taken with parsimony and caution, each dam is a unique work and must be analyzed individually, case by case. In other words, these simulations are based on a database of settlement Swedish box results and slab displacements, for a very specific example of a dam.

## Acknowledgements

The authors would like to thank the financial support of the Brazilian National Research Council (CNPq) and Post-Graduation Agency of Brazil (CAPES).

## Declaration of interest

The authors have no conflicts of interest to declare. All co-authors have observed and affirmed the contents of the paper and there is no financial interest to report.

## Authors' contributions

Renato Santos Paulinelli Raposo: conceptualization, data curation, visualization, software, investigation, methodology, writing – original draft. Yasletty Zamora Hernández: formal analysis, supervision, visualization, writing – original draft. André Pacheco de Assis: supervision, validation, writing – review and editing.

## List of symbols

<i>CFRD</i>	Concrete Face Rockfill Dams
<i>CR</i>	Settlement Swedish Boxes
<i>E</i>	Young's modulus
<i>S'</i>	Control variable for missing percentage of creep
<i>S</i>	Stress
<i>t</i>	Constructive time variable
<i>t<sub>f</sub></i>	Time constant at the end of construction
<i>t<sub>0</sub></i>	Construction start time constant
<i>U</i>	Total displacement

## References

- Basso, R.V. (2007). *Stress-strain study for one rockfill aiming concrete face rockfill dam* [Master's dissertation, University of São Paulo]. University of São Paulo's repository. <https://doi.org/10.11606/D.3.2007.tde-07082007-112420>.
- BSI BS 5975. (1996). *Code of practice for falsework friction*. British Standards Institution, London.
- Chen, Y., Gu, C., Shao, C., & Qin, X. (2019). Parameter sensitivity and inversion analysis for a concrete face rockfill dam based on CS-BPNN. *Advances in Civil Engineering*, 2019, 1-17. <http://dx.doi.org/10.1155/2019/9742961>.
- Cruz, P., Materón, B., & Freitas, M. (2014). *Barragens de enrocamento com face de concreto* (2. ed.). Oficina de Textos.
- Cruz, P.T., & Pereira, R.F. (2007). The rockfill of Campos Novos – CFRD. In *Proceedings of 3rd Symposium on Concrete Face Rockfill Dams* (pp. 207–216). Florianópolis, October 2007. CBDB.
- Frutuoso, A. (2007). *Análises tridimensionais de barragens de enrocamento com face de concreto com objetivo de otimizar os critérios de projeto* [PhD thesis, University of Brasília]. University of Brasília's repository (in Portuguese). <https://repositorio.unb.br/handle/10482/1582>.
- International Commission on Large Dams – ICOLD. (2010). *Concrete face rockfill dams: concepts for design and construction* (Bulletin 141). Paris.
- Naylor, D.J., Pande, G.N., Simpson, B., & Tabb, R. (1981). Finite element in geotechnical engineering. *International Journal for Numerical and Analytical Methods in Geomechanics*, 6(4), 491-492. <http://dx.doi.org/10.1002/nag.1610060409>.
- Oldecop, L.A., & Alonso, E.E. (2001). A model for rockfill compressibility. *Geotechnique*, 51(2), 127-139. <http://dx.doi.org/10.1680/geot.2001.51.2.127>.
- Oldecop, L.A., & Alonso, E.E. (2003). Suction effects on rockfill compressibility. *Geotechnique*, 53(2), 289-292. <http://dx.doi.org/10.1680/geot.2003.53.2.289>.
- Oldecop, L.A., & Alonso, E.E. (2007). Theoretical investigation of the time-dependent behaviour of rockfill. *Geotechnique*, 57(3), 289-301. <http://dx.doi.org/10.1680/geot.2007.57.3.289>.
- Pinto, N.L.S. (2007). Very high CFRDs: behaviour and design features. In *Proceedings of 3rd Symposium on Concrete Face Rockfill Dams* (pp. 43-49). Florianópolis, October 2007. CBDB.
- Pramthawee, P., Jongpradist, P., & Sukkarak, R. (2017). Integration of creep into a modified hardening soil model for time-dependent analysis of a high rockfill dam. *Computers and Geotechnics*, 91, 104-116. <http://dx.doi.org/10.1016/J.COMPGEO.2017.07.008>.
- Raposo, R.S.P. (2016). *Estudo tridimensional dos efeitos devido a força de percolação em barragens de enrocamento com face de concreto* [Master's dissertation, University of Brasília]. University of Brasília's repository (in Portuguese). <https://repositorio.unb.br/handle/10482/22604>.
- Sherard, L., & Cooke, B. (1987). Concrete-face rockfill dam: I. Assessment. *Journal of Geotechnical Engineering*, 113(10), 1096-1112. [http://dx.doi.org/10.1061/\(ASCE\)0733-9410\(1987\)113:10\(1096\)](http://dx.doi.org/10.1061/(ASCE)0733-9410(1987)113:10(1096)).
- Wei, K., & Zhu, S. (2015). Application of an elastoplastic model to predict behaviors of concrete-faced rockfill dam under complex loading conditions. *Journal of Civil Engineering and Management*, 21(7), 854-865. <https://doi.org/10.3846/13923730.2014.893911>
- Xavier, L.V., Albertoni, S.C., Antunes, J., Gasparetto, M., & Pereira, R.F. (2007). Concrete face rockfill dams-studies on face stresses through mathematical models.

- In *Proceedings of 3rd Symposium on Concrete Face Rockfill Dams* (pp. 129–138), Florianopolis, October 2007. CBDB.
- Yao, F., Guan, S., Yang, H., Chen, Y., Qiu, H., Ma, G., & Liu, Q. (2019). Long-term deformation analysis of Shuibuya concrete face rockfill dam based on response surface method and improved genetic algorithm. *Water Science and Engineering*, 12(3), 196-204. <http://dx.doi.org/10.1016/j.wse.2019.09.004>.
- Zhang, B., Wang, J.G., & Shi, R. (2004). Time-dependent deformation in high concrete-faced rockfill dam and separation between concrete face slab and cushion layer. *Computers and Geotechnics*, 31(7), 559-573. <http://dx.doi.org/10.1016/J.COMPGEO.2004.07.004>.
- Zhou, M.Z., Zhang, B.Y., & Jie, Y.X. (2016). Numerical simulation of soft longitudinal joints in concrete-faced rockfill dam. *Soil and Foundation*, 56(3), 379-390. <http://dx.doi.org/10.1016/J.SANDF.2016.04.005>.